



Effect of the sulfonated catalyst in obtaining biodiesel when used in a diesel engine with controlled tests

Efecto del catalizador sulfonado en la obtención de biodiesel cuando se usa en un motor diesel con pruebas controladas

L.A. Sánchez-Olmos^{1*}, M. Sánchez-Cárdenas¹, K. Sathish-Kumar², D.N. Tirado-González³, V.A. Maldonado-Ruelas¹, R.A. Ortiz-Medina⁴

¹Dirección de Postgrado e Investigación, Universidad Politécnica de Aguascalientes, Calle Paseo San Gerardo 207, Aguascalientes, C.P. 20342, Ags, México.

²Laboratorio de Cultivo de Tejidos Vegetales, Instituto Tecnológico El Llano Aguascalientes (ITEL)/ Tecnológico Nacional de México (TecNM). Km 18 carr. Aguascalientes-San Luis Potosí, El Llano Ags., C.P. 20330, México.

³INIFAP/CENID agricultura familiar. Km8.5 carretera Ojuelos-Lagos de Moreno, Ojuelos, Jalisco, México. CP. 47540.

⁴Ingeniería en energía, Universidad Politécnica de Aguascalientes, Calle Paseo San Gerardo 207, Aguascalientes, C.P. 20342, Ags, México.

Received: September 5, 2019; Accepted: November 7, 2019

Abstract

The experimentally obtained biodiesel from used vegetable oil is used as an alternative energy source that has been synthesized from reactions directed by a solid acid catalyst. The solid acid catalyst was prepared by sulfonating rubber from rubber for used tires. For the realization and analysis of biodiesel tests in the internal combustion engine, an experimental design was applied in which the type of biofuel feed was used as the main control, namely pure commercial diesel (DIEP), a mixture of 50/50% biodiesel-diesel (MEBD) and pure biodiesel (BIOP). The performance values and the emission and combustion characteristics of the fuel feed were investigated and compared under the same experimental conditions. During gas combustion, a considerable reduction of CO, unburned hydrocarbon and NOx emissions was achieved by using BIOP obtained in the laboratory compared to DIEP.

Keywords: Biodiesel, used oil, sulfonation, catalyst, atmospheric emission.

Resumen

El biodiesel obtenido experimentalmente del aceite vegetal usado se utilizó como una fuente de energía alternativa sintetizada a partir de reacciones dirigidas por un catalizador ácido sólido. El catalizador ácido sólido se preparó por sulfonación de carbón a partir de hule de neumáticos usados. Para la realización y el análisis de las pruebas de biodiesel en el motor de combustión interna se aplicó un diseño experimental en el que se utilizó el tipo de alimentación de biocombustible como factor de control principal, diesel comercial puro (DIEP), mezcla de biodiesel-diesel al 50/50% (MEBD) y biodiesel puro (BIOP). Los valores de rendimiento y las características de emisión y combustión de la alimentación de combustible se investigaron y compararon en las mismas condiciones experimentales. Durante la combustión gaseosa, se logró una reducción considerable de las emisiones de CO, hidrocarburos no quemados y NOx al usar BIOP obtenido en el laboratorio en comparación con DIEP.

Palabras clave: Biodiesel, aceite usado, sulfonación, catalizador, emisión a la atmósfera.

1 Introduction

Consequent from environmental problems and high costs of fossil fuels, companies, research

centers, and government agencies, are working on finding appropriate solutions. Hence, to avoid the consumption of fossil fuels that are considered as non-renewable energy (Evangelista-Flores *et al.*, 2014; Ahmadi *et al.*, 2013; Sánchez-Cárdenas *et al.*, 2016).

* Corresponding author. E-mail: luibandi_2000@hotmail.com

Tel. +52-449-106-83-95

<https://doi.org/10.24275/rmiq/IE831>

issn-e: 2395-8472

Further, to eliminate the environmental impacts caused by the depletion and usage of fossil fuels, several research groups are developing technology for the application of clean energy sources with high efficiencies, such as the solar energy, biomass, and wind that also helps in the development of the economy (Lubis *et al.*, 2011; Saleh *et al.*, 2011; Al-Nimr *et al.*, 2016; Sánchez-Cárdenas *et al.*, 2017; Sánchez-Roque *et al.*, 2019) in the transport sector. Combustion diesel engines are used because they show greater efficiency, more reliable and economically feasible because they allow significant fuel savings (Sadhik *et al.*, 2014; Peng *et al.*, 2018; Brusamarello *et al.*, 2019). However, it is time to search for the alternative renewable biodiesel as the efficient fuel that helps to minimize the excessive use of conventional diesel depends on the increase of need (Ramesh *et al.*, 2018; Wu *et al.*, 2017; Hosseini *et al.*, 2017). Regarding the regulatory framework, new regulations for the construction of diesel engines are updated and adapted, that allow complying with the regulations of atmospheric pollutants emitted by the combustion of diesel, and whose main objective is to take care of the environment (Efe *et al.*, 2018; Akar *et al.*, 2018).

In the last decades, a lot of alternative fuels have been developed, biodiesel is one of them, and they are also called methyl esters of vegetable/animal oils, which is considered as a viable substitute due to its lower impact with the environment, and this is derived from its high oxygen content and renewable nature (Zhang *et al.*, 2018; Emiroğlu *et al.*, 2018; Liu *et al.*, 2017). On the other hand, industrial needs to have been bordered on linking their processes with researchers, whose job is the search for new and more economic raw materials for obtaining biofuels with the focus of not to interfere with the economy of the necessary elements for human-edible use such as residual vegetable oils and animal fats (Chiatti *et al.*, 2018). As an option for the conversion of profitable renewable energies and based on previous and successful research reports to produce biofuels, this work based on waste vegetable oil collected from different restaurants in Mexico is considered as a promising source of raw material for the production of biodiesel (Liu *et al.*, 2017; Chiatti *et al.*, 2018; Faried *et al.*, 2017). Such a raw material comprising of vegetable oils and animal fats are composed of triglycerides, scientifically defined as esters of glycerol with long chains of fatty acids (Faried *et al.*, 2017; Mohamadzadeh *et al.*, 2017; Avinash *et al.*, 2018). The use of vegetable oil in the engine of Internal Combustion (IC) results in

carbon deposition and clogging of the injector in the combustion chamber of the engine. This issue can be minimized by reducing the viscosity of the oil by transesterification (Sun *et al.*, 2018). The transesterification of vegetable oil used with methyl alcohol and a solid acid catalyst, to obtain clean biodiesel of lower viscosity (Sánchez-Olmos *et al.*, 2017; Medina-Valtierra *et al.*, 2017). There have been widely applied in solid acid catalysts for biodiesel production (Niu *et al.*, 2018). Among various methods of solid acid catalysts, recently aroused the attention of biomass-derived solid acid catalysts. However, those solid acid catalysts are lack of surface area for the sulfonic acid anchor, as a result, hindering biodiesel production (Farabi *et al.*, 2019). In the present days, solid acid catalyst obtained from persistent materials such as used tires has a sustainable recyclable process (Sánchez-Olmos *et al.*, 2017). Industrially considering its production, biodiesel is obtained with the chemical process of transesterification where triglycerides react with an alcohol in the presence of an alkaline catalyst. In general, use of NaOH or KOH as catalyst is common for esterification and transesterification, however, it is difficult to separate, hence it made disadvantage. (Zhao *et al.*, 2018). These can occur in multiple reaction processes that include three reversible steps in series, where initially triglycerides are converted to diglycerides followed by the conversion of diglycerides to monoglycerides and in the final step, the monoglycerides are converted to esters and glycerol (Sonthalia *et al.*, 2019).

In the present work, methanol was used as an alkylating agent under conditions below the critical point in a homemade autogenous intermittent reactor and in the presence of a solid sulfonated carbon acid catalyst, by varying the quantity of catalyst, temperature and reaction time with the purpose of improving reaction efficiency, minimizing production costs comparing to diesel fuel (Sánchez-Olmos *et al.*, 2017; Medina-Valtierra *et al.*, 2017). In a previous study, biodiesel is utilized in a diesel engine where it was demonstrated that there is a decrease of pollutants exposed to the atmosphere during combustion (Sonthalia *et al.*, 2019). However, it is important to mention here that the inventors didn't make required modifications to the diesel engine for the testing of output power and emissions of engine pollutants like NO_x, CO, HC and smoke depending on the speed at which the steady-state conditions occur in an engine.

Table 1. Analysis of waste cooking.

Relative density	unit	value	Testing Procedure
Relative Density	g/ml	0.8503	ASTM D287
Free Fatty Acid	%	6.3	-
Kinematic Viscosity	cSt,40 °C	30.12	ASTM D445
Molecular Weight	g/mol	866.23	-
Saponification value	wt.%	188.21	ASTM D464

2 Materials and methods

2.1 Materials

The used vegetable oil was recollected from local restaurants in the city of Aguascalientes, Mexico. This raw material contains 0.45% free fatty acids, therefore considered suitable for use in the process of transesterification and obtaining biofuel discarding the esterification step (Sánchez-Olmos *et al.*, 2017; Czekala *et al.*, 2018). The viscosity values, acid and water content of the oil were determined according to the quality standard of the European Union (EN-14214). The result of these values is with a viscosity of 48.24 at 40 °C (mm²/s), an acid value of 0.27 (mg KOH/g) and a water content of 0.09 (% weight) and other data shown (Table 1). The oil was heated to 120 °C to remove excess water, and it was filtered to remove any solid residue before participating in the biodiesel production reactions. Anhydrous methanol (99.8%) was obtained from Sigma-Aldrich (Mexico). All the chemical products used were of analytical grade.

2.2 Preparation of sulfonated carbon catalyst

The preparation of the solid acid catalyst was began with a pyrolysis process, in which 5 g of ground tire rubber (pieces of 7.5 x 1.0 mm and 1 mm thick) was placed in a stainless steel reactor at a temperature of 500 °C with a heating ramp of 15 °C/min and N₂ flow of 30 ml/min for 2 h. At the end of the process, the carbonaceous material was obtained and washed to remove any impurities (Sánchez-Olmos *et al.*, 2017). For the sulfonation treatment, 10 g of carbon was taken and refluxed with 100 ml of concentrated H₂SO₄ at 140 °C for 12 h in a 500 ml flask. Then, the resulting suspension was washed with hot deionized water until reaching a neutral pH. After washing, it was subjected

to filtration and drying at 120 °C for 24 h in an oven to remove excess water. Finally, the sulfonated acid carbon catalyst was obtained.

2.3 Characterization of the catalysts

The sulfonated carbon was subjected to various physical and chemical characterizations, most of which were described in a previous document (Sánchez-Olmos *et al.*, 2017). The crystalline zones and the planes of the carbonaceous materials were determined by X-ray diffraction (XRD) using a Bruker diffractometer D8 model. The Raman spectra were obtained by a dispersive Micro-Raman JASCO NRS-5100 spectrophotometer. This equipment uses a laser diode wavelength of 532 nm and 30 mW of power (Elforlight G4-30; Nd: YAG). The total acidity and the resistance of the acid sites of the carbonaceous material were determined by thermally programmed desorption (TPD) of n-butylamine using a mass spectrometer model Prism placed in line. The adsorption/desorption tests were carried out in a quartz microreactor at atmospheric pressure using 0.2 g of a sample that was previously evacuated with He, under a flow of He/Ar saturated with n-butylamine at 0 °C. The total flow was 60 cm³/min, and the partial pressure of n-butylamine is 28.92 Torr. After that, the saturated sample was purged with pure He for 1 h to remove the trapped n-butylamine residue, and further, the desorption of n-butylamine was recorded by heating at 10 °C/min.

2.4 Transesterification of vegetable oil

The production of biodiesel was carried out using 60 ml of used vegetable oil which was mixed with 142 ml of anhydrous methanol along with 0.03% sulfonated carbonaceous catalyst at a temperature of 210 °C and a reaction time of 20 minutes. These reaction conditions are maintained constant in all experiments to obtain high-quality biodiesel (Medina-Valtierra *et al.*, 2017).

Table 2. Physicochemical properties and composition of Biodiesel.

Property	Unit	Biodiesel
Cloud point	°C	11.3
Pour pint	°C	7.9
Heating Value	MJ/Kg	41.1
Flash point	°C	163
Could point	°C	6
Density al 15 °C	Kg/m ³	794.9
Kinematic Viscosity	mm ² /s, 40 °C	4.211

The transesterification reaction was carried out in the closed stainless steel reactor (maximum capacity of 400 ml), a constant heating ramp of 20 °C/min was carried out starting from the room temperature until reaching the programmed temperature. Once the reactor reached the reaction temperature, it started the reaction time until it reached the programmed time. At the end of the reaction, the reactor was quickly cooled by placing it in a container with water at 20 °C, since the reaction is occurring at high temperatures (Hoque *et al.*, 2011). The properties of biodiesel are shown in Table 2.

2.5 Tests of biofuel in a diesel engine

The tests of power output and pollutant emissions of the engine such as NO_x, CO, HC and smoke depending on the speed were performed under steady-state conditions in a motor that operates with three speeds (1400, 1600, 1800 r/min). The main injection time was adjusted to the default engine configuration. The pilot injection was used at a constant engine speed of 1400 r/min, and the timing of the pilot and the injection process was also maintained constant. In the motor tests, three experimental runs were carried out where the DIEP was first evaluated (Mixture of paraffinic, olefinic and aromatic hydrocarbons, derived from crude oil processing). Afterward, the remaining two experiments were done firstly using MEBD where a mixture of 50% of diesel fuel and 50% of biodiesel were used and then the last test was carried out with BIOP obtained in the laboratory.

2.6 Engine test

The whole set of experiments was performed at the designed injection temperature of 23 °C, an injection pressure of 180 bar, the speed of 1500 RPM and a compression ratio of 17.5:1. The engine was started manually with DIEP fuel supply and was allowed

to reach it is steady-state (for about 10 minutes). The engine tests were carried out on a computerized platform of a single four-stroke diesel engine. It was directly coupled to a current dynamometer with a fixed position so that the motor can be maneuvered completely or partially. The motor and the dynamometer were interconnected with a control panel, which in turn was connected to a digital computer. The computer software 'Engine Analysis Software' was used to record the test parameters, such as the fuel flow rate, temperatures, airflow, load, etc. and to calculate the performance characteristics of the engine such as the thermal efficiency of the brake, the rate of heat release, etc. The experiments were performed at low and high fuel load. Subsequently, the engine was used with BIOP, DIEP, and MEBD to determine the analysis of each of them. For the analysis of the exhaust gases, the exhaust gas analyzer "AVL DITEST MDS 650" was used, whose specifications are given in Fig. 9 and to register the opacity of the smoke, the smoke meter "TESTO 338" was used.

2.7 Analysis of uncertainty

The uncertainties of the parameters were calculated by sequential perturbation. Some of the average uncertainties of the measured and calculated parameters are airflow (1.1%), liquid fuel flow (0.1%), gas flow (2%), engine load (0.1%), engine speed (1.3%), cylinder pressure (0.8%), temperature (1.0%) and lower calorific value (LCV) of the liquid fuel (1.0%). Based on this, the calculated accuracy of the performance and the combustion studies of the engine are within ± 4.6%. However, the accuracy of the emission study is ± 4.6%. The maximum variance coefficient values of the performance parameters, i.e., Brake Thermal Efficiency (BTE) and Brake specific fuel (BSFC) are 3% and 4% respectively. While the parameters of combustion emission, namely, Peak

Cylinder Pressure, Ignition Delay, CO, HC, and NOx have shown VOC of 5, 4, 2, 2, and 6% respectively (Özener *et al.*, 2014).

3 Results and discussion

3.1 Physicochemical characterization of carbonaceous materials

The elemental carbon composition of tire rubber has an amount of elemental S caused by the vulcanization of the tire rubber. Further, subjecting this to a pyrolysis treatment it maintains an amount of elemental sulfur in the carbon (Tovar-Martinez *et al.*, 2018). The quantification of the total acidity density in the catalytic support and the sulfonated carbon (CAS) sample was carried out by the acid-base titration method resulting in a density of acid groups of 0.92 mmol/g (non-sulfonated) and 2.82 mmol/g (sulfonated). The carbon structure gave results similar to those presented by Tang *et al.*, 2019 and Lathiya *et al.*, 2018. The thermal stability of the CAS was analyzed by TGA under nitrogen flow as shown in Fig. 1.

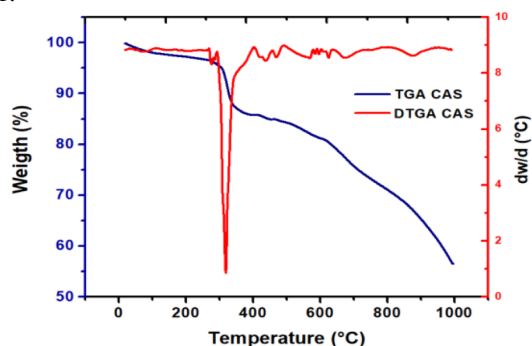


Fig. 1. CAS thermogravimetry analysis.

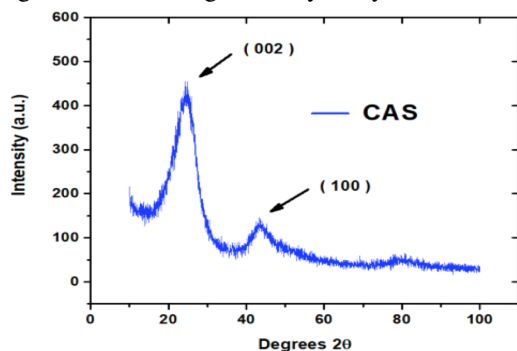


Fig. 2. The sulfonated carbon-based material XRD pattern.

The CAS exhibits three transition zones. The first region extends between 36-320 °C, where the mass loss is about 4.8% by weight attributed to the release of physically bound water and probably a loss of -OH groups. The second transition at 400-750 °C is attributed to the decomposition of the remaining organic groups, together with the collapse of the amorphous carbon structure. Above 500 °C, the acid group (COOH) and other functional groups are eliminated (Lu *et al.* 2008). In the third stage, the disintegration appears in the range of high temperatures typically between 700-950 °C, due to the existence and stability of the covalent bond between the sulfonic acid site (-SO₃H) and the carbon surface (Bezerra *et al.*, 2014; Devi *et al.*, 2017). The XRD patterns of the CAS are shown in Fig. 2.

The diffractograms show two main peaks 2θ around 25.5 ° and 43.6 °. The first peak (plane 002) can be indexed to graphene in nanosheets in disorder and the second one is attributed to the plane (100) of graphite. These results indicate the presence of graphitic carbon. Materials such as ZnO and CaCO₃ that are used for the vulcanization/polymerization process during the manufacture of vehicle tires were not detected in XRD as this has been suggested by other works (Alves *et al.*, 2012; Wang *et al.*, 2018). Impurity materials were removed after sulfonic treatment, and that has considerably improved the main peaks outlined above. This is inconsistent with the amorphous carbon materials mentioned in previous reports (Gopinath *et al.*, 2017). The surface area and porosity presented in CAS presented in Table 3, the total BET area and the pore volume of the CAS sample was decreased. It could be speculated that the sulfuric acid treatment process eliminates impurities and compounds not subject to the structure of carbon. As a result of this, there is a decrease in total pore volume, and the specific volume of mesopores is generated.

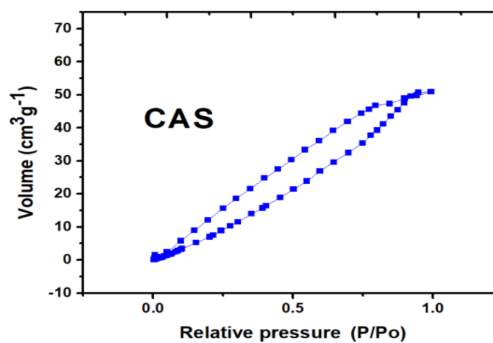


Fig. 3. Isotherm of the CAS sample. Adsorption of N₂; closed symbols, desorption of N₂.

Table 3. Textural parameters of the original and sulfonated carbons.

Sample	Specific surface, SBET (m ² /g)	Pore volume, VP (cm ³ /g)	Pore average size, DP (nm)	Mesopore specific volume (cm ³ /g)
C (non Sulfonated)	115.943	0.403	14.112	0.373
CAS	97.99	0.319	18.669	0.307

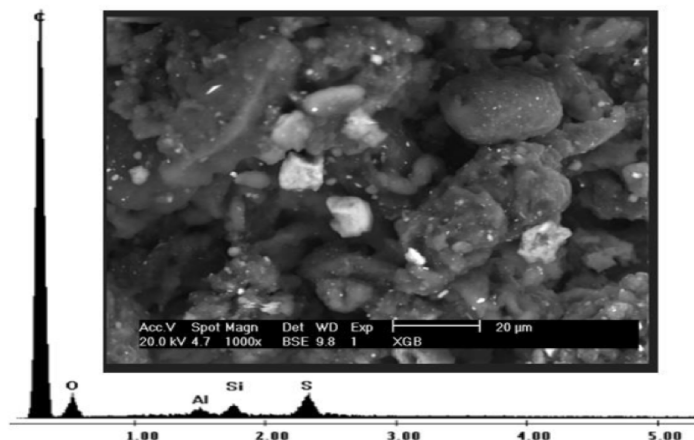


Fig. 4. SEM and EDX analysis of sulfonated carbon.

The adsorption isotherms are of type II, with a mesoporous volume between 0.20 and 0.30 cm³/g. Two groups of mesopores were detected in the samples, considering the IUPAC classification, which defines mesopores as pores with diameters between 2 nm and 50 nm. A small number of narrow mesopores (3.6 and 4.3 nm) close to being considered as micropores (< 2 nm) were found in the CAS sample. The second group of relatively large mesopores (18.3-18.4 nm) was also detected, as seen in the graphs shown in Fig. 3.

The SEM image of the CAS sample is shown in Fig. 4. This acid catalyst is turned out to be constituted by particles of different and irregular sizes with a diameter of 3-40 μm. However, the large aggregate particles could be formed due to agglomeration during the sulfonation treatment by solid-state reactions.

The EDXs analyzes of the CAS sample were carried out to determine its chemical composition in weight percentage and atomic percentage. Fig. 4. is the SEM scan of the sulfonated carbon powder where the EDXs scan is obtained. The elemental analysis found increase of sulfonation carbon of 214.6% (wt%) (Sánchez-Olmos *et al.*, 2017). The EDX analysis also confirms the presence of a significant amount of S. The minimum emission voltage value of S

was approximately 2.36 keV. This analysis showed an increase in the amount of C and S in sulfonated carbon, as shown in Fig. 4. It was observed that the original carbon contains 1.78% S and in sulfonated carbon (acid catalyst) 3.82% S was observed, which shows a remarkable increase in S after the sulfonation process. From the chemical composition in CAS, it can be concluded that for 200 carbon atoms (C), there are approximately 3 and 6, Sulfur (S) and Oxygen (O) atoms respectively present on the catalyst surface.

The IR spectrum of CAS (Fig. 5.) shows a first peak located at 617 cm⁻¹ with a weak intensity corresponding to the S-O bond according to the data reported in the literature (Hou *et al.*, 2012). A vibratory peak at 726 cm⁻¹ corresponds to the aromatic residue with average intensity. An IR signal at 1254 cm⁻¹ with a weak intensity corresponds to the aromatic bond C-C. One of the most important IR peaks is located at 1074 cm⁻¹ having strong intensity assigned to the acid groups -SO₃H and represented by the symmetric vibration of O = S = O (Farabi *et al.*, 2019), other IR peaks in which carbon atoms are involved in 1447 cm⁻¹ and 1717 cm⁻¹ with strong and average intensities corresponding to the functional group C = C and the conjugated C = O group respectively (dos Santos *et al.*, 2018).

Table 4. Different processes used for the conversion of oils into biodiesel.

S. No	Feedstock	Catalyst	FAME Yield	Ref.
1	Palm fatty acid	sulfonated carbon-based	94.20%	Farabi <i>et al.</i> 2019
2	Corn acid oil	orange peels-sulfonated	91.68%	Lathiyat <i>et al.</i> 2018
3	Levulinic acid	Carbon sulfonated	88.30%	Özener <i>et al.</i> 2017
4	Waste cooking oil	Carbon sulfonated	95.80%	Farabi <i>et al.</i> 2019
5	Waste cooking oil	Carbon sulfonated	94.50%	Medina-Valtierra <i>et al.</i> 2017

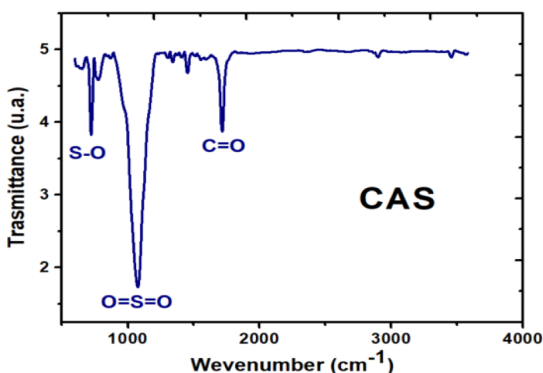


Fig. 5. IR spectroscopy of CAS.

The quantification of acidity and the definition of the acid resistance in the CAS catalyst was also obtained from the integration of the curves in the analysis of the thermal desorption of n-butylamine on the surface of the CAS, resulting in the following acid values; CAS = 2.78 mmol g⁻¹. It defines a large number of acid groups in the sulfonated carbon strongly anchored in the carbon layer (dos Santos *et al.*, 2018; Ogino *et al.*, 2018).

3.2 Transesterification of waste vegetable oil

After the transesterification reaction to produce biodiesel with CAS catalyst in the autogenous reactor, the remaining solution was decanted to remove the catalyst and glycerin was formed. Then, the methanol was recovered by evaporation at 70 °C (Sánchez-Olmos *et al.*, 2017). The reaction was brought to 240 °C using a molar ratio of methanol to the oil of 24:1, a mass ratio of catalyst to the oil of 0.1, and a reaction time of 20 min. A pressure reached 900 psi and temperatures in the reactor played an important role in reactivity to transesterification reactions under subcritical methanol conditions. The biodiesel yield was 95.69% by volume for the CAS sample. A good result obtained from the gas chromatography analysis was a high content of FAME in the biodiesel produced,

more than 80% by weight. Different catalysts used to obtain biodiesel are shown in Table 4.

3.3 Effects of the reaction parameters

The parameters of biodiesel production are crucial, which reflects the performance even more. The main parameters analyzed were the amount of catalyst (W), temperature (T) and reaction time (t). In general, deactivation of the catalyst resulted from contact between the oil and methanol in the reaction mixture (Amani *et al.*, 2014). To verify the optimization model, Box-Behnken was applied, in order to determine the best reaction conditions (T=210°C, t=20min and Catalyst amount (W)=0.03 wt%) yielding the following: The combination of factor levels is obtained, with a maximum equivalent yield of 95.69% of biodiesel, in the indicated region, which is 210 °C, 20 min and 0.03% by weight of the catalyst. From these statistical studies, it is suggested that the model proposed by Medina-Valtierra *et al.*, 2017 and Sánchez-Olmos *et al.*, 2017, is adequate to predict the conversion rate of TG in the field of the variables investigated.

Fig. 6. shows the behavior of renewable biodiesel obtained from a sulfonated catalyst in a diesel engine with the best conditions based on the design of biodiesel experiments (BIOP) (Sánchez-Olmos *et al.*, 2017), as well as the output power for renewable biodiesel compatible in a mixture of biodiesel-diesel 50/50 (MEBD) and commercial diesel (DIEP).

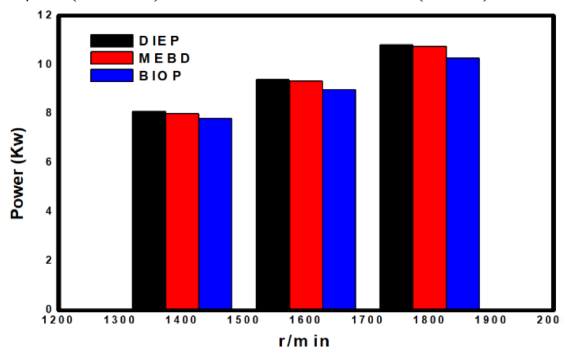


Fig. 6. Power output for BIOP, MEBD, and DIEP.

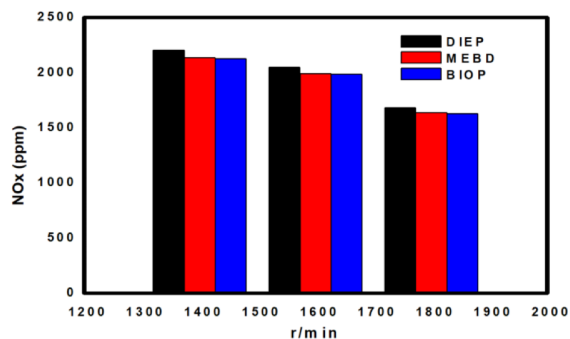


Fig. 7. NOx emission for BIOP, MEBD, and DIEP.

When comparing BIOP, DIEP, and MEBD, a minimum output power variation was detected, around 2% variation between each sample. The value of the calorific value of biodiesel is responsible for this reduction (Pinzi *et al.*, 2013). Some authors reported similarity in this behavior in 100% for gas and Partial Biodiesel loads (Varatharajan *et al.*, 2012) where they mention a 5% power reduction and are attributed to the calorific value of biodiesel. Likewise, it can be attributed to the reduction of potency to the oxygens present in the biodiesel molecule (Olikara *et al.*, 2010; Deng *et al.*, 2017; Jiaqiang *et al.*, 2018). The DIEP starts before the MEBD and the BIOP at the time of combustion. These behaviors are attributed to a brief ignition delay as well as an advanced injection time for the MEBD and BIOP samples since these two samples containing biodiesel have a higher density and higher kinematic viscosity (Ban-Weiss *et al.*, 2007; Westbrook *et al.*, 2018).

Fig. 7. shows the analysis of the composition of NOx present in the emissions at different speeds, considering in the first instance that the NOx emissions are sensitive to the oxygen content present in the combustion mixture in the adiabatic flame, which is referred to the temperature and pulverization of the fuel inside the engine (Qi *et al.*, 2009). To considering the physical characteristics of the fuel injection studied, NOx production can be modified, such as the size of the fuel drop, the degree of mixing of air and fuel inside the combustion chamber, the evaporation rate, the geometry of the engine, among others (Monyem *et al.*, 2001). The samples of BIOP, DIEP, and MEBD analyzed in the diesel engine showed a decrease in NOx by increasing the engine speed as when using the DIEP and MEBD samples. This is truncated to the increase in volumetric efficiency and gas flow within the combustion chamber (Suresh *et al.*, 2015).

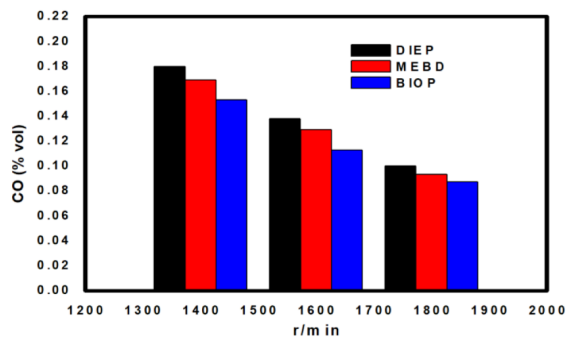


Fig. 8. CO emission for BIOP, MEBD, and DIEP.

Likewise, considering that the molecule of the obtained biodiesel has a higher oxygen content compared to commercial diesel, reacting with the air of the nitrogen-containing mixture results in a greater NOx production upon reaction (Diya'Uddeen *et al.*, 2012; Patel *et al.*, 2016).

Fig. 8. Shows the quantities of CO emissions from the BIOP, MEBD and DIEP fuels. In this test, it was observed that when increasing the speed of the engine, the formation of CO decreased. This is attributed to the decrease of the coefficient of the excess of air, and to better combustion and evaporation of the fuel by the temperature and pressure of injection in the cylinder (Monyem *et al.*, 2001). The production of CO as an intermediate product of the process is affected mainly by the composition of gas mixtures and temperature (Mohan *et al.*, 2015). This decrease in the amount of CO can also be attributed to the oxygen content in BIOP, MEBD, and DIEP due to poor atomization (Roskilly *et al.*, 2008). The DIEP fuel produced a higher CO emission compared to the BIOP; this is attributed to the oxygen present in the BIOP molecule, causing better combustion of the molecule at high temperatures in the cylinder (Dharmadhikari *et al.*, 2012; Özener *et al.*, 2014).

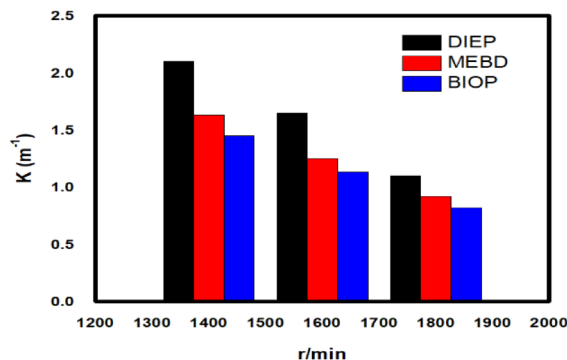


Fig. 9. Smoke emission for BIOP, MEBD, and DIEP.

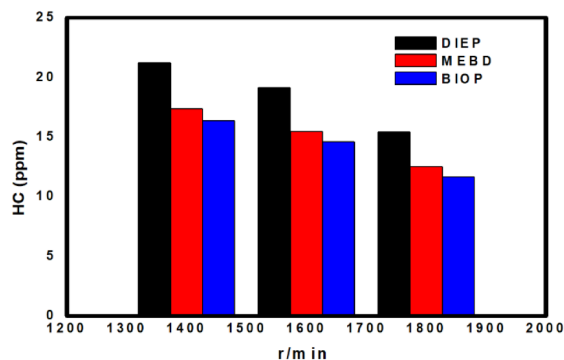


Fig. 10. HC emission for BIOP, MEBD, and DIEP.

Fig. 9. shows the smog opacity (K), lower K values were obtained in the BIOP, MEBD samples compared to the DIEP sample. With samples containing biodiesel, it showed a K decrease of 22% for MEBD and 31% for BIOP compared to DIEP. The value of K is formed due to incomplete combustion (Manigandan *et al.*, 2019). This issue is because biodiesel has oxygen in the molecule, which causes better combustion and fewer soot formation (Abed *et al.*, 2018).

The variations of HC emissions are shown in Fig. 10. The results obtained show a reduction of the HC emissions with the increase of the engine load for the samples of BIOP, DIEP, and MEBD used in the diesel engine. As a first feature of the analyzed samples, the BIOP gives a lower emission of HC compared to the DIEP and approximately a midpoint, the MEBD showed. This behavior is attributed to the fact that there is better combustion in the presence of the biodiesel molecule in the samples. Since it contains oxygen atoms at the end of the chain, causing better combustion in the engine (Shehata *et al.*, 2014; Mufrodi *et al.*, 2018). The amount is also taken into account of cetans present in the BIOP which causes a decrease in HC emissions due to the delay caused when starting the diesel engine (Qi *et al.*, 2009; Monyem *et al.*, 2001). When using the MEBD sample, it showed an 18% reduction in HC average compared to DIEP, and the BIOP sample showed a reduction of 23% in average HC compared to DIEP.

Conclusions

The CAS material resulting from the production above processes showed to be an efficient catalyst for the transesterification of the used vegetable oil. From

this, we can mention that the treatment with sulfuric acid can eliminate the impurities in the surface and promote in the surface of the carbon with a union of sulphonyl groups possessing strong acid character. The heterogeneous catalyst used in this study showed a good performance in the production of methyl esters and was easy to separate from the liquid mixture. The highest rate of conversion of triglycerides was 96.51% indicated in previous works. This behavior occurred at the reaction conditions for a temperature reaction of 210 °C, a reaction time of 20 min and a catalyst amount of 0.03% by weight. The results obtained in the engine with BIOP, MEBD, and DIEP showed that the kinematic viscosity and the relationship between the FMAE are important factors. With the increase of C18:1, C18:0 and C16:0 the physical ignition is delayed, as well as C16:0, because a higher kinematic viscosity does not favor the mixture of fuel and air, evaporation of the fuel and the efficiency of combustion. Therefore, the physical and chemical ignition delay collectively affects the general ignition time. DIEP produced fewer NOx emissions and the lower power indicated by producing the highest HC and CO emissions. However, better performance and emission characteristics were observed with BIOP, although it showed an increase in NOx emissions. Comparing with DIEP, BIOP due to its low caloric value and higher kinematic viscosity showed a slightly deficient performance in its characteristics. Compared to DIEP, at low loads, CO and HC emissions increase by 5%, but significantly decrease by approximately 30% at medium and high load, while, at low load, there is an increase of 5% at NOx emissions, but at medium and high loads are reduced by approximately 30%. The oxygen content of biodiesel is beneficial and improves combustion in the cylinder at high loads.

Nomenclature

DIEP	Commercial Diesel
MEBD	Mixture Of Biodiesel-Diesel 50/50
BIOP	Biodiesel
IC	Internal Combustion
LCV	Lower Calorific Value
BTE	Brake Thermal Efficiency
CAS	Sulfonated Carbon
FAME	Fatty Acid Methyl Ester
W	Catalyst
T	Temperature
t	Reaction Time

References

- Abed, K. A., El Morsi, A. K., Sayed, M. M., Shaib, A. A. E., & Gad, M. S. (2018). Effect of waste cooking-oil biodiesel on performance and exhaust emissions of a diesel engine. *Egyptian Journal of Petroleum* 27, 985-989. <https://doi.org/10.1016/j.ejpe.2018.02.008>
- Ahmadi, P., Dincer, I., & Rosen, M. A. (2013). Development and assessment of an integrated biomass-based multi-generation energy system. *Energy* 56, 155-166. <https://doi.org/10.1016/j.energy.2013.04.024>
- Akar, M. A., Kekilli, E., Bas, O., Yildizhan, S., Serin, H., & Ozcanli, M. (2018). Hydrogen enriched waste oil biodiesel usage in compression ignition engine. *International Journal of Hydrogen Energy* 43, 18046-18052. <https://doi.org/10.1016/j.ijhydene.2018.02.045>
- Al-Nimr, M. A., Kiwan, S. M., & Talafha, S. (2016). Hybrid solar-wind water distillation system. *Desalination* 395, 33-40. <https://doi.org/10.1016/j.desal.2016.05.018>
- Alves, C. T., De Oliveira, A. S., Carneiro, S. A. V., Santos, R. C. D., Vieira De Melo, S. A. B., Andrade, H. M. C., Marques, F. C., & Torres, E. A. (2012). Transesterification of waste frying oils using ZnAl₂O₄ as heterogeneous catalyst. *Procedia Engineering* 42, 1928-1945. <https://doi.org/10.1016/j.proeng.2012.07.589>
- Amani, H., Ahmad, Z., Asif, M., & Hameed, B. H. (2014). Transesterification of waste cooking palm oil by MnZr with supported alumina as a potential heterogeneous catalyst. *Journal of Industrial and Engineering Chemistry* 20, 4437-4442. <https://doi.org/10.1016/j.jiec.2014.02.012>
- Avinash, A., & Murugesan, A. (2018). Judicious recycling of biobased adsorbents for biodiesel purification: a critical review. *Environmental Progress and Sustainable Energy*, 1-8. <https://doi.org/10.1002/ep.13077>
- Ban-Weiss, G. A., Chen, J. Y., Buchholz, B. A., & Dibble, R. W. (2007). A numerical investigation into the anomalous slight NO_x increase when burning biodiesel; A new (old) theory. *Fuel Processing Technology* 88, 659-667. <https://doi.org/10.1016/j.fuproc.2007.01.007>
- Bezerra, K. S., & Antoniosi Filho, N. R. (2014). Gas chromatographic analysis of free steroids in biodiesel. *Fuel* 130, 149-153. <https://doi.org/10.1016/j.fuel.2014.04.024>
- Brusamarello, C.Z., Di Domenico, M., Da Silva, C., de Castilhos F. (2019) A comparative study between multivariate calibration and artificial neural network in quantification of soybean biodiesel. *Revista Mexicana de Ingeniería Química* 19, 123-132.
- Chiatti, G., Chiavola, O., & Palmieri, F. (2018). Impact of waste cooking oil in biodiesel blends on particle size distributions from a city-car engine. *Journal of the Energy Institute* 91, 262-269. <https://doi.org/10.1016/j.joei.2016.11.009>
- Czekała, W., Bartnikowska, S., Dach, J., Janczak, D., Smurzyńska, A., Kozłowski, K., Bugała, A., Lewicki, A., Cieślík, M., Typańska, D., & Mazurkiewicz, J. (2018). The energy value and economic efficiency of solid biofuels produced from digestate and sawdust. *Energy* 159, 1118-1122. <https://doi.org/10.1016/j.energy.2018.06.090>
- Deng, Y., Zheng, W., Jiaqiang, E., Zhang, B., Zhao, X., Zuo, Q., Zhang, Z., & Han, D. (2017). Influence of geometric characteristics of a diesel particulate filter on its behavior in equilibrium state. *Applied Thermal Engineering* 123, 61-73. <https://doi.org/10.1016/j.applthermaleng.2017.05.071>
- Devi, A., Das, V. K., & Deka, D. (2017). Ginger extract as a nature based robust additive and its influence on the oxidation stability of biodiesel synthesized from non-edible oil. *Fuel* 187, 306-314. <https://doi.org/10.1016/j.fuel.2016.09.063>
- Dharmadhikari, H. M., Kumar, P. R., & Rao, S. S. (2012). Performance and emissions of C.I. engine using blends of biodiesel and diesel at different injection pressures. *International Journal of Applied Research in Mechanical Engineering*

- 2, 2231-5950. Retrieved from <https://pdfs.semanticscholar.org/a97e/229a26d90ec39915ae9104ab35f62d57bf1b.pdf>
- Diya'Uddeen, B. H., Abdul Aziz, A. R., Daud, W. M. A. W., & Chakrabarti, M. H. (2012). Performance evaluation of biodiesel from used domestic waste oils: A review. *Process Safety and Environmental Protection* 90, 164-179. <https://doi.org/10.1016/j.psep.2012.02.005>
- dos Santos, V. H. J. M., Pestana, V. Z., de Freitas, J. S., & Rodrigues, L. F. (2018). A preliminary study on traceability of biodiesel mixtures based on the raw materials profiles from Brazilian regions and fourier transform infrared spectroscopy (FTIR). *Vibrational Spectroscopy* 99, 113-123. <https://doi.org/10.1016/j.vibspec.2018.09.005>
- Efe, Ş., Ceviz, M. A., & Temur, H. (2018). Comparative engine characteristics of biodiesels from hazelnut, corn, soybean, canola and sunflower oils on DI diesel engine. *Renewable Energy* 119, 142-151. <https://doi.org/10.1016/j.renene.2017.12.011>
- Emiroğlu, A. O., Keskin, A., & Şen, M. (2018). Experimental investigation of the effects of turkey rendering fat biodiesel on combustion, performance and exhaust emissions of a diesel engine. *Fuel* 216, 266-273. <https://doi.org/10.1016/j.fuel.2017.12.026>
- Evangelista-Flores, A., Alcántar-González, F. S., Cruz-Gómez, M. J., Ramírez de Arellano Aburto, N., Cohen Barki, A., & Robledo-Pérez, J. M. (2014). Design of a continuous process of biodiesel production. *Revista Mexicana de Ingeniería Química* 13, 483-491.
- Farabi, M. S. A., Ibrahim, M. L., Rashid, U., & Taufiq-Yap, Y. H. (2019). Esterification of palm fatty acid distillate using sulfonated carbon-based catalyst derived from palm kernel shell and bamboo. *Energy Conversion and Management* 181, 562-570. <https://doi.org/10.1016/j.enconman.2018.12.033>
- Faried, M., Samer, M., Abdelsalam, E., Yousef, R. S., Attia, Y. A., & Ali, A. S. (2017). Biodiesel production from microalgae: Processes, technologies and recent advancements. *Renewable and Sustainable Energy Reviews*. <https://doi.org/10.1016/j.rser.2017.05.199>
- Gopinath, S., Kumar, P. S. M., Arafath, K. A. Y., Thiruvengadaravi, K. V., Sivanesan, S., & Baskaralingam, P. (2017). Efficient mesoporous SO₄²⁻/Zr-KIT-6 solid acid catalyst for green diesel production from esterification of oleic acid. *Fuel* 203, 488-500. <https://doi.org/10.1016/j.fuel.2017.04.090>
- Hoque, M. E., Singh, A., & Chuan, Y. L. (2011). Biodiesel from low cost feedstocks: The effects of process parameters on the biodiesel yield. *Biomass and Bioenergy* 35, 1582-1587. <https://doi.org/10.1016/j.biombioe.2010.12.024>
- Hosseini, S. H., Taghizadeh-Alisarai, A., Ghobadian, B., & Abbaszadeh-Mayvan, A. (2017). Effect of added alumina as nano-catalyst to diesel-biodiesel blends on performance and emission characteristics of CI engine. *Energy* 124, 543-552. <https://doi.org/10.1016/j.energy.2017.02.109>
- Hou, K., Zhang, A., Gu, L., Liu, M., & Guo, X. (2012). Efficient synthesis and sulfonation of ordered mesoporous carbon materials. *Journal of Colloid and Interface Science* 377, 18-26. <https://doi.org/10.1016/j.jcis.2012.03.029>
- Jiaqiang, E., Zhang, Z., Chen, J., Pham, M. H., Zhao, X., Peng, Q., Zhang, B., & Yin, Z. (2018). Performance and emission evaluation of a marine diesel engine fueled by water biodiesel-diesel emulsion blends with a fuel additive of a cerium oxide nanoparticle. *Energy Conversion and Management* 169, 194-205. <https://doi.org/10.1016/j.enconman.2018.05.073>
- Lathiya, D. R., Bhatt, D. V., & Maheria, K. C. (2018). Synthesis of sulfonated carbon catalyst from waste orange peel for cost effective biodiesel production. *Bioresource Technology Reports* 2, 69-76. <https://doi.org/10.1016/j.biteb.2018.04.007>
- Liu, H., Ma, X., Li, B., Chen, L., Wang, Z., & Wang, J. (2017). Combustion and emission characteristics of a direct injection diesel engine

- fueled with biodiesel and PODE/biodiesel fuel blends. *Fuel* 209, 62-68. <https://doi.org/10.1016/j.fuel.2017.07.066>
- Lu, A. H., Spliethoff, B., & Schüth, F. (2008). Aqueous synthesis of ordered mesoporous carbon via self-assembly catalyzed by amino acid. *Chemistry of Materials* 20, 5314-5319. <https://doi.org/10.1021/cm800362g>
- Lubis, L. I., Kanoglu, M., Dincer, I., & Rosen, M. A. (2011). Thermodynamic analysis of a hybrid geothermal heat pump system. *Geothermics* 40, 233-238. <https://doi.org/10.1016/j.geothermics.2011.06.004>
- Manigandan, S., Gunasekar, P., Devipriya, J., & Nithya, S. (2019). Emission and injection characteristics of corn biodiesel blends in diesel engine. *Fuel* 235, 723-735. <https://doi.org/10.1016/j.fuel.2018.08.071>
- Medina-Valtierra, J., Sánchez-Olmos, L. A., Carrasco-Marin, F., & Sánchez-Cárdenas, M. (2017). Optimization models type box-behnken in the obtaining of biodiesel from waste frying oil using a large-acidity carbonaceous catalyst. *International Journal of Chemical Reactor Engineering* 15, 1-15. <https://doi.org/10.1515/ijcre-2017-0072>
- Mohamadzadeh Shirazi, H., Karimi-Sabet, J., & Ghotbi, C. (2017). Biodiesel production from Spirulina microalgae feedstock using direct transesterification near supercritical methanol condition. *Bioresource Technology* 239, 378-386. <https://doi.org/10.1016/j.biortech.2017.04.073>
- Mohan, B., Tay, K. L., Yang, W., & Chua, K. J. (2015). Development of a skeletal multi-component fuel reaction mechanism based on decoupling methodology. *Energy Conversion and Management* 105, 1223-1238. <https://doi.org/10.1016/j.enconman.2015.08.060>
- Monyem, A., Van Gerpen, J. H., & Canakci, M. (2001). The effect of timing and oxidation on emissions from biodiesel-fueled engines. *Transactions of the American Society of Agricultural Engineers* 44, 35-42.
- Mufrodi, Z., Budiman, A., & Purwono, S. (2018). Operation conditions in syntesize of bioaditive from glycerol as by-product biodiesel: a review. *Energy Procedia* 145, 434-439. <https://doi.org/10.1016/j.egypro.2018.04.071>
- Niu S, Ning Y, Lu C, et al (2018) Esterification of oleic acid to produce biodiesel catalyzed by sulfonated activated carbon from bamboo. *Energy Convers Manag.* doi: [10.1016/j.enconman.2018.02.055](https://doi.org/10.1016/j.enconman.2018.02.055)
- Ogino, I., Suzuki, Y., & Mukai, S. R. (2018). Esterification of levulinic acid with ethanol catalyzed by sulfonated carbon catalysts: Promotional effects of additional functional groups. *Catalysis Today* 314, 62-69. <https://doi.org/10.1016/j.cattod.2017.10.001>
- Olikara, C., & Borman, G. L. (2010). A computer program for calculating properties of equilibrium combustion products with some applications to I.C. engines. *SAE Technical Paper Series*, 1. <https://doi.org/10.4271/750468>
- Özener, O., Yüksek, L., Ergenç, A. T., & Özkan, M. (2014). Effects of soybean biodiesel on a DI diesel engine performance, emission and combustion characteristics. *Fuel* 115, 875-883. <https://doi.org/10.1016/j.fuel.2012.10.081>
- Patel, P. D., Lakdawala, A., Chourasia, S., & Patel, R. N. (2016). Bio fuels for compression ignition engine: A review on engine performance, emission and life cycle analysis. *Renewable and Sustainable Energy Reviews* 65, 24-43. <https://doi.org/10.1016/j.rser.2016.06.010>
- Peng, Q., E, J., Zhang, Z., Hu, W., & Zhao, X. (2018). Investigation on the effects of front-cavity on flame location and thermal performance of a cylindrical micro combustor. *Applied Thermal Engineering* 130, 541-551. <https://doi.org/10.1016/j.applthermaleng.2017.11.016>
- Pinzi, S., Rounce, P., Herreros, J. M., Tsolakis, A., & Pilar Dorado, M. (2013). The effect of biodiesel fatty acid composition on combustion and diesel engine exhaust emissions. *Fuel* 104, 170-182. <https://doi.org/10.1016/j.fuel.2012.08.056>
- Qi, D. H., Geng, L. M., Chen, H., Bian, Y. Z., Liu, J., & Ren, X. C. (2009). Combustion and

- performance evaluation of a diesel engine fueled with biodiesel produced from soybean crude oil. *Renewable Energy* 34, 2706-2713. <https://doi.org/10.1016/j.renene.2009.05.004>
- Ramesh, D. K., Dhananjaya Kumar, J. L., Hemanth Kumar, S. G., Namith, V., Basappa Jambagi, P., & Sharath, S. (2018). Study on effects of alumina nanoparticles as additive with poultry litter biodiesel on performance, combustion and emission characteristic of diesel engine. *Materials Today: Proceedings* 5, 1114-1120. <https://doi.org/10.1016/j.matpr.2017.11.190>
- Roskilly, A. P., Nanda, S. K., Wang, Y. D., & Chirkowski, J. (2008). The performance and the gaseous emissions of two small marine craft diesel engines fuelled with biodiesel. *Applied Thermal Engineering* 28, 872-880. <https://doi.org/10.1016/j.applthermaleng.2007.07.007>
- Sadhik Basha, J., & Anand, R. B. (2014). Performance, emission and combustion characteristics of a diesel engine using carbon nanotubes blended Jatropha methyl ester emulsions. *Alexandria Engineering Journal* 53, 259-273. <https://doi.org/10.1016/j.aej.2014.04.001>
- Saleh, A., Qudeiri, J. A., & Al-Nimr, M. A. (2011). Performance investigation of a salt gradient solar pond coupled with desalination facility near the Dead Sea. *Energy* 36, 922-931. <https://doi.org/10.1016/j.energy.2010.12.018>
- Sánchez-Cárdenas, M., Medina-Valtierra, J., Kamaraj, S. K., Trejo-Zárraga, F., & Antonio Sánchez-Olmos, L. (2017). Physicochemical effect of Pt nanoparticles/ γ - Al_2O_3 on the oleic acid hydrodeoxygenation to biofuel. *Environmental Progress and Sustainable Energy*. <https://doi.org/10.1002/ep.12563>
- Sánchez-Cárdenas, M., Medina-Valtierra, J., Kamaraj, S.-K., Medina Ramírez, R., & Sánchez-Olmos, L. (2016). Effect of size and distribution of ni nanoparticles on γ - Al_2O_3 in oleic acid hydrodeoxygenation to produce n-alkanes. *Catalysts*. <https://doi.org/10.3390/catal6100156>
- Sánchez-Olmos, L. A., Medina-Valtierra, J., Sathish-Kumar, K., & Sánchez Cardenas, M. (2017). Sulfonated char from waste tire rubber used as strong acid catalyst for biodiesel production. *Environmental Progress and Sustainable Energy*. <https://doi.org/10.1002/ep.12499>
- Sánchez-Roque Y., Pérez-Luna, Y., Moreira-Acosta J., Farrera-Vázquez N., Sebastian J., Berrones Hernández R. (2019). Optimization for the production of verrucodesmus verrucosus biomass through crops in autotrophic and mixotrophic conditions with potential for the production of biodiesel. *Revista Mexicana de Ingeniería Química* 19, 133-146
- Shehata, M. S., Elkotb, M. M., & Salem, H. (2014). Combustion characteristics for turbulent prevaporized premixed flame using commercial light diesel and kerosene fuels. *Journal of Combustion*, 2014. <https://doi.org/10.1155/2014/363465>
- Sonthalia, A., & Kumar, N. (2019). Hydroprocessed vegetable oil as a fuel for transportation sector: A review. *Journal of the Energy Institute* 92, 1-17. <https://doi.org/10.1016/j.joei.2017.10.008>
- Sun, Y., Zhang, J., Sun, Z., & Zhang, L. (2018). Biodiesel production using calcium-based catalyst from venus shell: Modeling of startup production in an industrial reactor. *Environmental Progress and Sustainable Energy* 1-9. <https://doi.org/10.1002/ep.13053>
- Suresh, M., Prakash, R. H., & Prasad, B. D. (2015). Internal combustion engines - A comprehensive study, 4, 220-224.
- Tang, X., & Niu, S. (2019). Preparation of carbon-based solid acid with large surface area to catalyze esterification for biodiesel production. *Journal of Industrial and Engineering Chemistry* 69, 187-195. <https://doi.org/10.1016/j.jiec.2018.09.016>
- Tovar-Martinez, E., Moreno-Torres, J. A., Cabrera-Salazar, J. V., Reyes-Reyes, M., Chazaror Ruiz, L. F., & López-Sandoval, R. (2018). Synthesis of carbon nano-onions doped with nitrogen using spray pyrolysis. *Carbon* 140,

- 171-181. <https://doi.org/10.1016/j.carbon.2018.08.056>
- Varatharajan, K., & Cheralathan, M. (2012). Influence of fuel properties and composition on NO x emissions from biodiesel powered diesel engines: A review. *Renewable and Sustainable Energy Reviews*, 16(6), 3702-3710. <https://doi.org/10.1016/j.rser.2012.03.056>
- Wang, A., Li, H., Pan, H., Zhang, H., Xu, F., Yu, Z., & Yang, S. (2018). Efficient and green production of biodiesel catalyzed by recyclable biomass-derived magnetic acids. *Fuel Processing Technology* 181, 259-267. <https://doi.org/10.1016/j.fuproc.2018.10.003>
- Westbrook, C. K., Sjöberg, M., & Cernansky, N. P. (2018). A new chemical kinetic method of determining RON and MON values for single component and multicomponent mixtures of engine fuels. *Combustion and Flame* 195, 50-62. <https://doi.org/10.1016/j.combustflame.2018.03.038>
- Wu, Q., Xie, X., Wang, Y., & Roskilly, T. (2017). Experimental investigations on diesel engine performance and emissions using biodiesel adding with carbon coated aluminum nanoparticles. *Energy Procedia* 142, 3603-3608. <https://doi.org/10.1016/j.egypro.2017.12.251>
- Zhang, Z., E, J., Deng, Y., Pham, M. H., Zuo, W., Peng, Q., & Yin, Z. (2018). Effects of fatty acid methyl esters proportion on combustion and emission characteristics of a biodiesel fueled marine diesel engine. *Energy Conversion and Management* 159, 244-253. <https://doi.org/10.1016/j.enconman.2017.12.098>
- Zhao, C., Yang, L., Xing, S., Luo, W., Wang, Z., & Lv, P. (2018). Biodiesel production by a highly effective renewable catalyst from pyrolytic rice husk. *Journal of Cleaner Production* 199, 772-780. <https://doi.org/10.1016/j.jclepro.2018.07.242>